Article

The Antimicrobial Peptide CRAMP-34 Eradicates *Escherichia coli* Biofilms by Interfering with the *kduD*-Dependent Network

Hongzao Yang , Jing Xiong , Sisi Su , Zhuo Yang , Wu Yang , Lianci Peng , Suhui Zhang , Jinjie Qiu , Yuzhang He , Hongwei Chen *

Posted Date: 19 December 2025

doi: 10.20944/preprints202512.1811.v1

Keywords: *Escherichia coli*; *kduD*; Biofilm; CRAMP-34; eradicate

 doi:10.20944/preprints202512.1811.v1

Article

The Antimicrobial Peptide CRAMP-34 Eradicates *Escherichia coli* Biofilms by Interfering with the *kduD*-Dependent Network

Hongzao Yang [1,2,3,†], Jing Xiong [1,†], Sisi Su [1], Zhuo Yang [1], Wu Yang [4], Lianci Peng [1], Suhui Zhang [2,5], Jinjie Qiu [2,5], Yuzhang He [1] and Hongwei Chen [1,2,3,*]

[1] College of Veterinary Medicine, Southwest University, Chongqing 402460, China
[2] National Center of Technology Innovation for Pigs, Chongqing 402460, China
[3] Chi Institute of Traditional Chinese Veterinary Medicine, Southwest University, Chongqing 402460, China
[4] Dali Jinming Animal Pharmaceutical Co., Ltd 671006, China
[5] Chongqing Academy of Animal Sciences, Chongqing 402460, China
* Correspondence: dyxchw@swu.edu.cn
† These authors contributed equally to this work.

Abstract

Background/Objectives: Bacterial biofilms formed by *Escherichia coli* pose a significant challenge in veterinary medicine due to their intrinsic resistance to antibiotics. Antimicrobial peptides (AMPs) represent a promising alternative. AMPs exert their bactericidal activity by binding to negatively charged phospholipids in bacterial membranes via electrostatic interactions, leading to membrane disruption and rapid cell lysis. **Methods**: In vitro assays included MIC determination, biofilm eradication testing (crystal violet, colony counts, CLSM), swimming motility, and EPS quantification. CRISPR/Cas9 was used to construct and complement a *kduD* mutant. A transposon mutagenesis library was screened for biofilm-defective mutants. In vivo, a murine excisional wound infection model was treated with CRAMP-34, with wound closure and bacterial burden monitored. Gene expression changes were analyzed via RT-qPCR. **Results:** The mouse-derived AMP (abbreviation CRAMP-34) effectively eradicates pre-formed biofilms of a clinically relevant, porcine-origin *E.coli* strain and promotes wound healing in a murine infection model. We conducted a genome-wide transposon mutagenesis screen, which identified *kduD*, as a critical gene for robust biofilm formation. Functional characterization revealed that *kduD* deletion drastically impairs flagellar motility and alters exopolysaccharide production, leading to defective biofilm architecture without affecting growth. Notably, the anti-biofilm activity of CRAMP-34 phenocopied aspects of the *kduD* deletion, including motility inhibition and transcriptional repression of a common set of biofilm-related genes. **Conclusions:** The research highlight CRAMP-34 as a potent anti-biofilm agent and unveil *kduD* as a previously unrecognized regulator of *E.coli* biofilms development, whose associated pathway is implicated in the mechanism of action of CRAMP-34.

Keywords: *Escherichia coli*; *kduD*; Biofilm; CRAMP-34; eradicate

1. Introduction

Escherichia coli (*E. coli*) causes persistent diarrhea and antimicrobial resistance due to its propensity to form aggressive and dense bacterial biofilms [1]. The bacteria in biofilms secrete various components, such as extracellular polymeric substances (EPS), that cause bacterial accumulation with multiple layers and protect the embedded cells against antimicrobial agents and host immune defense, prompting biofilm-associated infections (BAI) [2]. Previous studies have reported that the tolerance of biofilms to various antibiotics is 10–1000 times greater than that of planktonic cells [3].The

 doi:10.20944/preprints202512.1811.v1

life cycle of biofilms includes the following stages: reversible/irreversible adhesion, formation, maturation, and dispersion. In the initial attachment, flagella and fimbriae facilitate mechanical attachment to the surface. With increasing cell density, the autoinducer concentration reaches a threshold, and the autoinducer/regulatory protein (the receptor) complex induces or represses the expression of target genes [4]. Pili-mediated twitching motility and a high concentration of cyclic diguanylic acid (c-di-GMP) enable the attached cells to aggregate to form microcolonies within self-produced EPS, thereby ensuring the adherence of the bacteria to the surface of a thickly complex bio-molecular layer [5]. The fully matured biofilms have a typical three-dimensional mushroom-like structure. This formulates a highly structured biofilms that is difficult to eradicate.

They have shown that genes directly involved in the biofilms formation of *E.coli* include synthetic operon pgaABCD for Poly-β-1,6-N-acetyl-d-glucosamine (poly-β-1,6-GlcNAc; PGA), glycogen synthesis operon *glgCAP*, autoaggregation adhesin Artigen 43, gene *wza* for synthesizing multimeric outer membrane protein complex, the operons *bcsABZC* and *bcsEFG* encoding cellulose synthase complex, and operons *csgBAC* and *csgDEFG* for the curli fimbriae protein synthesis and assembly [6–8]. Another study showed that more than 60 genes are directly involved in the regulation of *E.coli* biofilms formation via signal transduction pathways, such as quorum sensing (QS) system, second messenger c-di-GMP system, two-component regulatory system (TCS), transcription regulatory proteins, and non-coding small RNAs(sRNAs) [9–11]. Nonetheless, whether there are new regulatory genes in E.coli biofilms formation is yet to be investigated.

Our studies have shown that the mouse cathelicidins related antimicrobial peptide (abbreviation CRAMP-34) inhibits biofilms formation and eradicates the mature biofilms in the biofilms model strain *Pseudomonas aeruginosa* [12]. However, whether CRAMP-34 has the same inhibitory effect on *E.coli* biofilms is yet to be clarified. In addition, the key regulatory genes for biofilms formation and maturation in *E.coli* also need to be explored further. Therefore, the current study focused on a strain of *E.coli* isolated from a porcine source with strong biofilms formation ability carrying the mobilized colistin resistance (*mcr*) gene.

Despite the well-characterized roles of operons such as *bcsABZC* and *csgDEFG* in biofilms formation, the complete genetic network regulating this process in *E.coli* remains incompletely understood. To systematically identify novel regulators, we employed a functional screen using transposon mutagenesis. This approach, combined with subsequent CRISPR/Cas9-mediated validation, led to the identification of an unreported key gene, *kduD*, encoding 2-dehydro-3-deoxy-D-gluconate 5-dehydrogenase (*KduD*), as a critical regulator of biofilms formation in this strain. Furthermore, given the central role of *KduD*, we investigated its potential as a target for anti-biofilm agents and specifically evaluated whether it mediates the anti-biofilm effect of the antimicrobial peptide CRAMP-34.

2. Results

2.1. CRAMP-34 Demonstrates Potent Biofilm-Eradicating Activity and Promotes Wound Healing In Vivo

Different concentrations of CRAMP-34 were used on 1-day-old preformed biofilms, ciprofloxacin (CIP) and human antibacterial peptide LL-37 were used as controls. The MIC values of CRAMP-34 and LL-37 were 7.8125 μg/mL and 15.625 μg/mL, respectively, and that of CIP is 0.015625 μg/mL. The results of crystal violet staining showed that CRAMP-34 and CIP significantly reduce the biomass of *Ec*032 biofilms at the concentration of 4× MIC–64× MIC. However, CRAMP-34 exerted a significant effect on reducing the biomass of Ec032 biofilms at 16× MIC with a rate of 92.95% (Figure 1 A). The results of the colony counting assay showed that CRAMP-34 killed more biofilms than LL-37 and CIP, and the biofilms decreased by 2.76 log values with a killing rate of 99.83% at 16× MIC (Figure 1 B).

To visualize the anti-biofilm activity of CRAMP-34, SYTO 9 (living) and propidium iodide (PI) (dead) staining was performed under the CLSM. As shown in Figure 1 C–F, the CRAMP-34 intervention group biofilms were significantly reduced compared to *Ec*032. The results showed that CRAMP-34 remarkedly reduced *Ec*032 biofilms at a concentration of 125 μg/mL, decreasing the

 doi:10.20944/preprints202512.1811.v1

number (75.90%), volume (97.69%), and base area (8.69%) (Figure 1 H–I). Furthermore, the fluorescence intensity of SYTO 9 and PI bacteria decreased by 89.11% and 92.28%, respectively (Figure 1 J). In addition, the ratio of fluorescence intensity of SYTO 9 and PI per unit base area of biofilms decreased by 88.09% ($P<0.01$) and 91.63% ($P<0.01$), respectively (Figure 1 K), and the ratio of fluorescence intensity of SYTO 9 and PI per unit volume of biofilms increased by 77.68% ($P<0.01$) and 70.91% ($P<0.01$), respectively (Figure 1 L).

The wound of each group of mice was photographed regularly to observe the healing process. As shown in Figure 1 M, compared with the PBS group,the wound healing rate in the CRAMP-34 treatment group was significantly accelerated, and the wound area was significantly reduced. Residual bacteria at the wound site were sampled daily and counted by the plate method. Compared with the PBS group, the number of bacterial colonies in the CRAMP-34 treatment group was significantly reduced (Figure 1 N), and the relative wound closure rate was increasingly smaller, both with significant differences, which further verified the antibacterial effect of CRAMP-34 (Figure 1 O). In summary, CRAMP-34 significantly promoted the healing of wounds caused by *E.coli*.

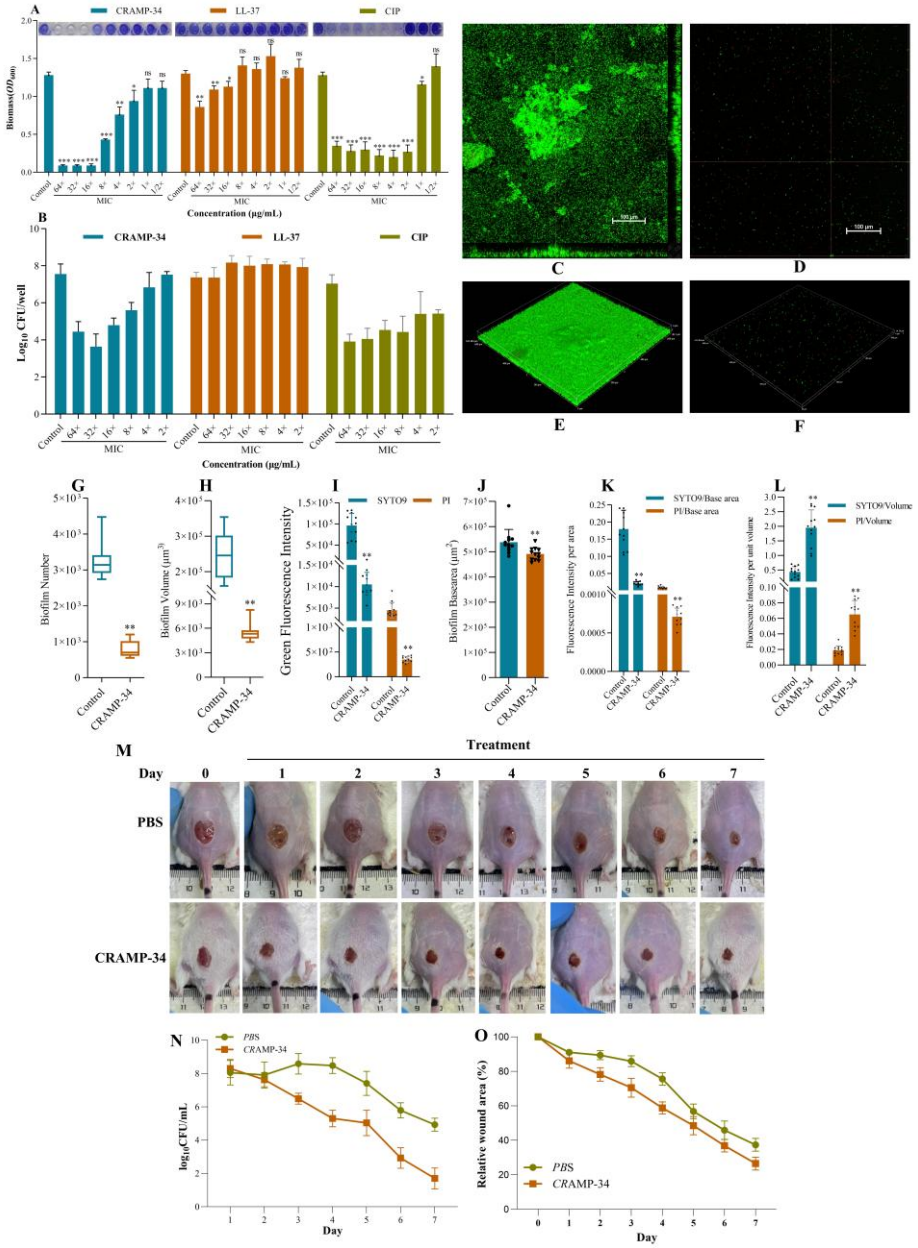

Figure 1. CRAMP-34 demonstrates potent biofilm-eradicating activity and promotes wound healing in vivo. (A) The biomass of *Ec*032 biofilms (1-day-old) treated with CRAMP-34, LL-37, and CIP was detected by crystal violet

 doi:10.20944/preprints202512.1811.v1

staining. (B) The viable bacteria of *Ec*032 biofilms (1-day-old) treated with CRAMP-34, LL-37, and CIP was detected by crystal violet staining. (C) and (D) The orthogonal views and three-dimensional biofilms representation under the 20× objective in the control group. (E) and (F) The orthogonal views and three-dimensional biofilms representation of CRAMP-34 in the objective of 20×. (G) Biofilm Number. (H) Biofilm volume. (I) The fluorescence intensity of live and dead bacteria. (J) Biofilms basearea. (K) The fluorescence intensity per unit area (fluorescence intensity / base area). (L) Fluorescence intensity per unit volume (fluorescence intensity / volume). (M) Representative wound photos of mice from different treatment groups. (O) antibacterial efficacy of different treatments that are determined by the results of bacterial colony counts. (N) Statistics of wound shrinkage rates.

2.2. A Genome-Wide Screen Identifies kduD as a Novel Gene Essential for Robust Biofilm Formation

A random mariner transposon mutagenesis library of *Ec*032, comprising 141,667 mutants, was constructed to identify genes involved in biofilms formation. From this library, 25 independent mutants exhibiting a pronounced reduction in biofilms were isolated (Figure 2 A). Subsequent phenotypic characterization via the Congo red assay revealed that these mutants collectively displayed a loss of colony wrinkling, a transition to a smoother morphology, and diminished pigmentation compared to the wild-type *Ec*032 and an empty vector control strain (*Ec*032Δ) (Figure 2 B). ERIC-PCR analysis confirmed that all 25 strains were genuine transposon mutants, ruling out contamination (Figure 2 C). Whole-genome sequencing and comparative analysis pinpointed the transposon insertion site in all mutants to a single specific locus, which we designated as *kduD* (Figure 2 D).

To definitively establish the role of *kduD* in biofilms formation, an in-frame deletion mutant (*Ec*032Δ*kduD*) was generated using the CRISPR/Cas9 system (Figure 2 E), with its identity verified by Sanger sequencing and electrophoretic analysis (Figure 2 F-G). The deletion of *kduD* had no discernible impact on bacterial growth kinetics (Figure 2 H). However, quantitative assessment of biofilms formation using crystal violet staining demonstrated a significant impairment in the *Ec*032Δ*kduD* mutant across multiple time points. The most severe defect, a reduction of 60.13%, was observed at 9 h. This phenotype was successfully complemented, as biofilms formation were restored to near wild-type levels when the mutant was transformed with a plasmid carrying the *kduD* gene (pBAD24-*kduD*) (Figure 2 I).

Further analysis using the Congo red-binding assay indicated that the deletion of *kduD* did not abolish the production of curli fimbriae and cellulose, key biofilm matrix components, and the colony morphology of the defined mutant was distinct from the initial transposon mutants (Figure 2 J). Intriguingly, quantification of EPS revealed a significant increase in EPS production in the *Ec*032Δ*kduD* mutant at equivalent bacterial densities (Figure 2 K).These results demonstrated that *kduD* plays a critical role in mediating biofilms formation.

Collectively, these findings demonstrate that *kduD* is a key regulator of biofilm development in *Ec*032, likely through a mechanism involving the modulation of EPS production.

 doi:10.20944/preprints202512.1811.v1

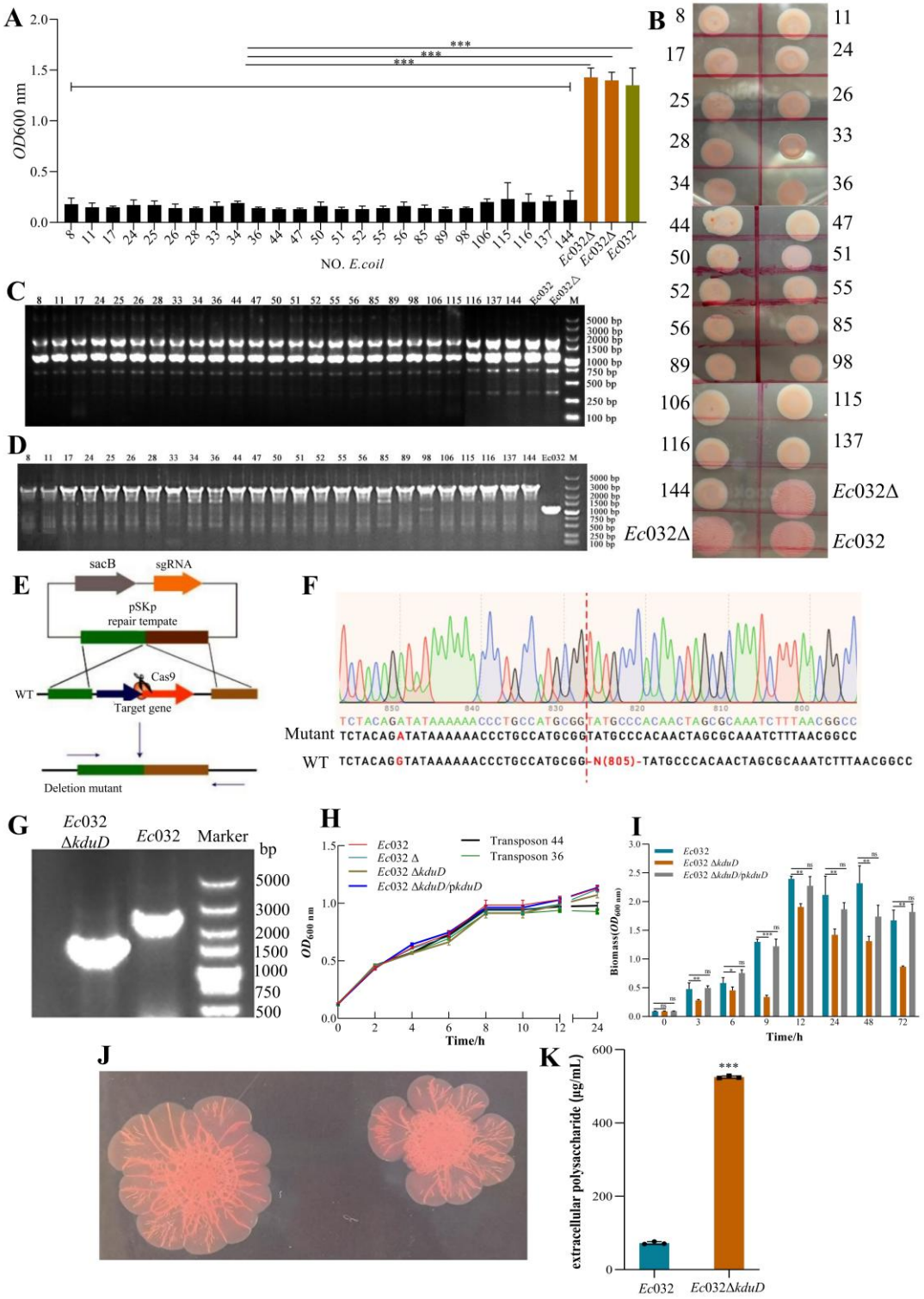

Figure 2. Identification of *kduD* through transposon mutagenesis and its role in biofilms formation, colony morphology, and EPS production in *Ec*032. (A) Biomass of mutant biofilms (1-day-old) in 96-well plates was detected by crystal violet staining. (B) Congo red observation of colony morphology in *Ec*032-related mutant strains. (C) Electrophoretogram of ERIC-PCR. (D) Identification of transposon insertion sites in mutant strains. (E) Schematic diagram of the pCasKp-OriT/pSGKp system construction process. (F) Peak map of Sanger sequence. (G) Electrophoretogram. (H) Growth curves of various bacterial strains. (I) Biomass (1-day-old) were treated in the test tube by crystal violet staining. (J) Congo red colony morphology. (K) The content of EPS at the same bacterial level.

 doi:10.20944/preprints202512.1811.v1

2.3. kduD Regulates Biofilm by Modulating Flagellar Motility and EPS Production

Swimming and twitching motility assays were used to investigate the flagella and pili movement of biofilms. The results showed that the swimming motility of planktonic and biofilms cells in *Ec*032Δ*kduD* was decreased by 46.43% and 77.46% (Figure 3 A), and the twitching motility was decreased by 32.50% and 36.17%, respectively (Figure 3 B). These results suggested that *kduD* mediates the formation of *E.coli* biofilms by regulating motility.

CLSM was utilized to observe the effect of *kduD* deletion on biofilms formation. As shown in Figure 2C–F, *Ec*032Δ*kduD* biofilms were significantly reduced compared to *Ec*032. In addition, *Ec*032Δ*kduD* could not affect the number and base area (Figure 3 G-H), but significantly reduced the volume and cube surface of biofilms (Figure 3 I-J).

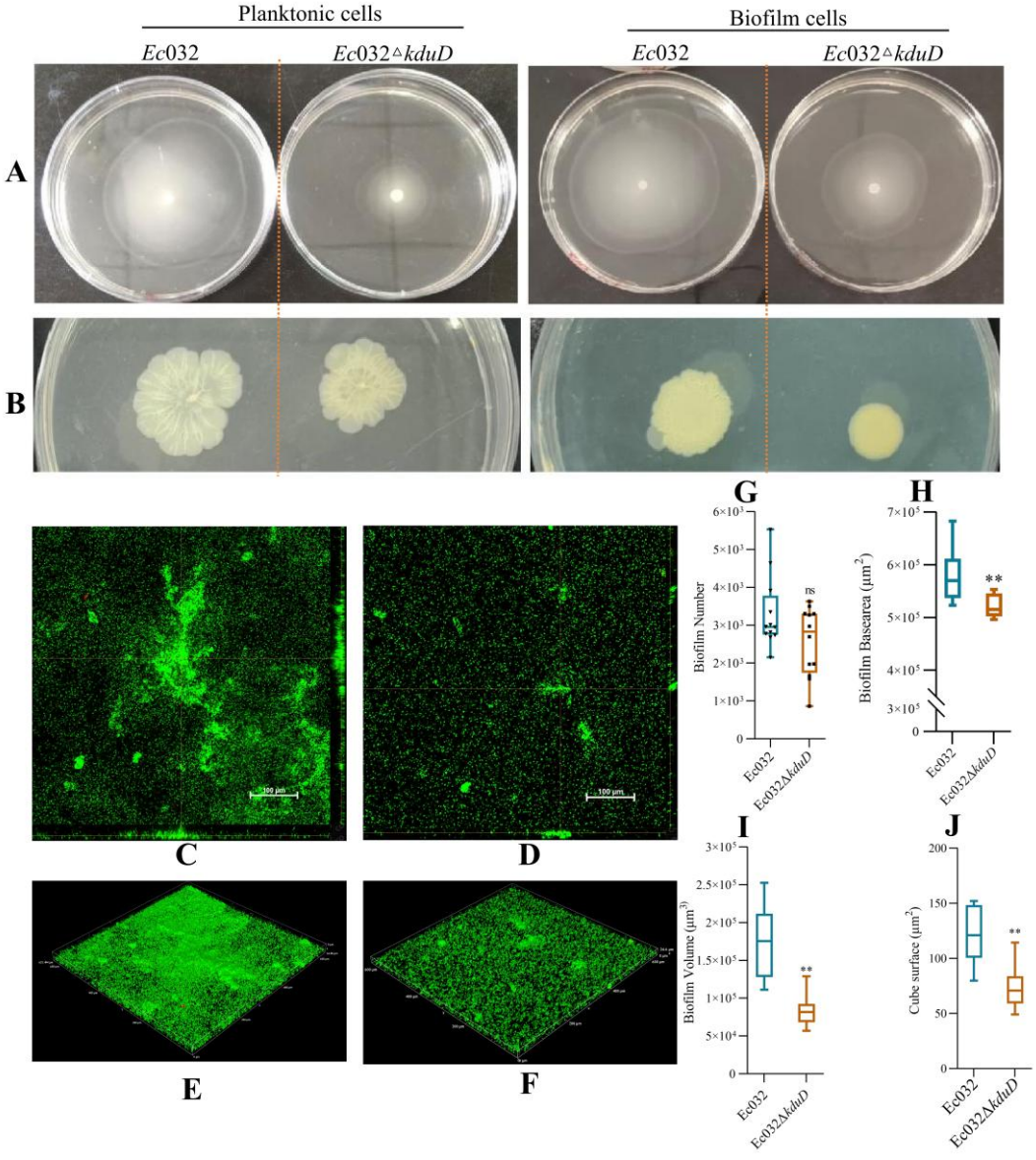

Figure 3. *kduD* regulates biofilm architecture by modulating flagellar motility and exopolysaccharide production. (A) Swimming zone diameter. (B) Twitching zone diameter. (C) and (D) The orthogonal views and three-dimensional biofilms representation under 20× in the *Ec*032 group. (E) and (F) The orthogonal views and three-dimensional biofilms representation under 20× in the *Ec*032Δ*kduD* group. (G) Biofilms number. (H) Biofilm basearea. (I) Biofilm volume. (J) Cube surface of biofilms.

We found that the mRNA expression levels of the biofilm-related genes in *Ec*032Δ*kduD* were upregulated compared to *Ec*032, as assessed by RT-qPCR. These biofilm-related genes included

 doi:10.20944/preprints202512.1811.v1

flagella-related genes (*fliE*, *fliA*, *motA*, *motB*, and *ycgR*) (Figure 4 A), adhesion-related genes (*csgD* and *bcsA*) (Figure 4 B), QS-related genes (*luxS*, *lsrK*, *qseC*, and *qseB*) (Figure 4 C), TCS-related genes (*phoP*, *rcsA*, *rcsB* and *cpxR*) (Figure 4 C), and *kduD*-related genes (*uxaA*, *uxuA*, *yqeF*, *araE* and *ygeA*) (Figure 4 D). These results demonstrated that *kduD* plays a critical role in mediating biofilms formation.

Moreover, the mRNA expression levels of biofilm-related genes in CRAMP-34-treated *Ec*032 and *Ec*032Δ*kduD* by RT-qPCR. The results showed that the mRNA levels of the related genes, such as flagella-related genes (*flhD*, *flhC*, *fliE*, *fliA*, *motA*, *motB*, and *ycgR*) (Figure 4 A), adhesion-related genes (*csgD* and *bcsA*, except *fimA* and *papG*) (Figure 4 B), QS-related genes (*luxS*, *lsrK*, *qsEc*, and *qseB*) (Figure 4 C), TCS-related genes (*phoP*, *phoQ*, *basR*, *rcsA* and *rcsB*, except *basS* and *cpxR*) (Figure 4 D), and *kduD*-related genes (*uxaA*, *uxuA*, *yqeF*, *kduD*, *araE* and *ygeA*) (Figure 4 E), were downregulated after the intervention of CRAMP-34 with *Ec*032 and *Ec*032Δ*kduD*. These results indicated that the scavenging effect of CRAMP-34 on mature biofilms of *E.coli* is related to EPS and *kduD* metabolic pathway.

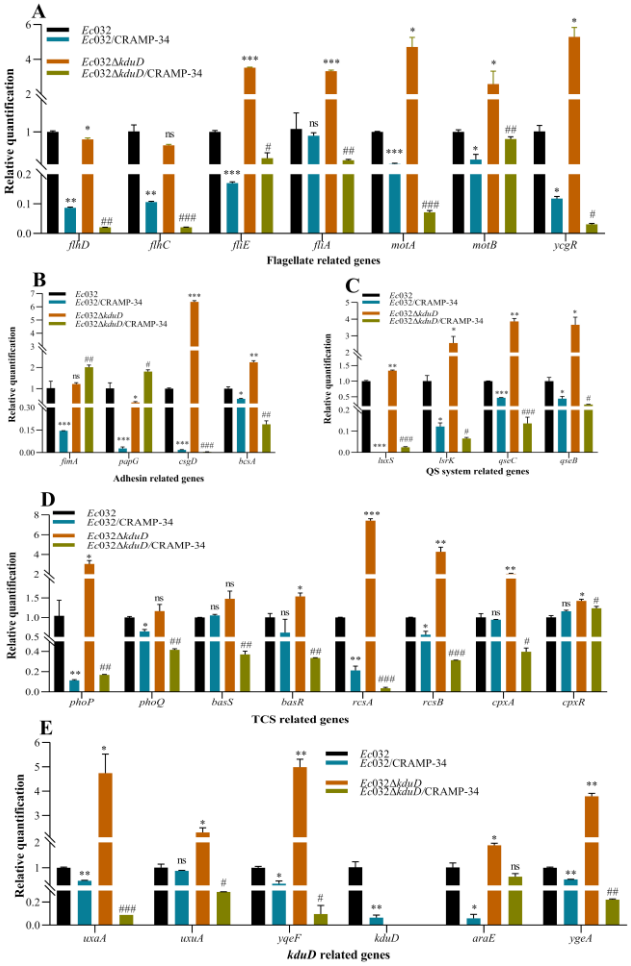

Figure 4. Relative expression of the biofilm-associated genes. (A) The mRNA level of flagellate-related genes. (B) The mRNA level of adhesin-related genes. (C) The mRNA level of QS system-related genes. (D) The mRNA level of TCS system-related genes. (E) The mRNA level of *kduD*-related genes. Data are expressed as the mean ± SD of three independent experiments. Note.* $P < 0.05$, ** $P < 0.01$, *** $P < 0.001$ compared to the nontreated *Ec*032 group. # $P < 0.05$, ## $P < 0.01$, ### $P < 0.001$ compared to the nontreated *Ec*032Δ*kduD* group.

The results of crystal violet staining revealed that the inhibition rate of biofilms of CRAMP-34 on *Ec*032Δ*kduD* was decreased at all concentrations compared to *Ec*032 (Figure 5 A). The effect of CRAMP-34 on the flagella motility of *Ec*032 and *Ec*032Δ*kduD* was observed by spotting planktonic and biofilms cells liquid onto agar plate containing different concentrations of CRAMP-34. The results showed that CRAMP-34 inhibits the flagellar movement that recovers gradually with the decreased concentration of CRAMP-34 (Figure 5 B).

 doi:10.20944/preprints202512.1811.v1

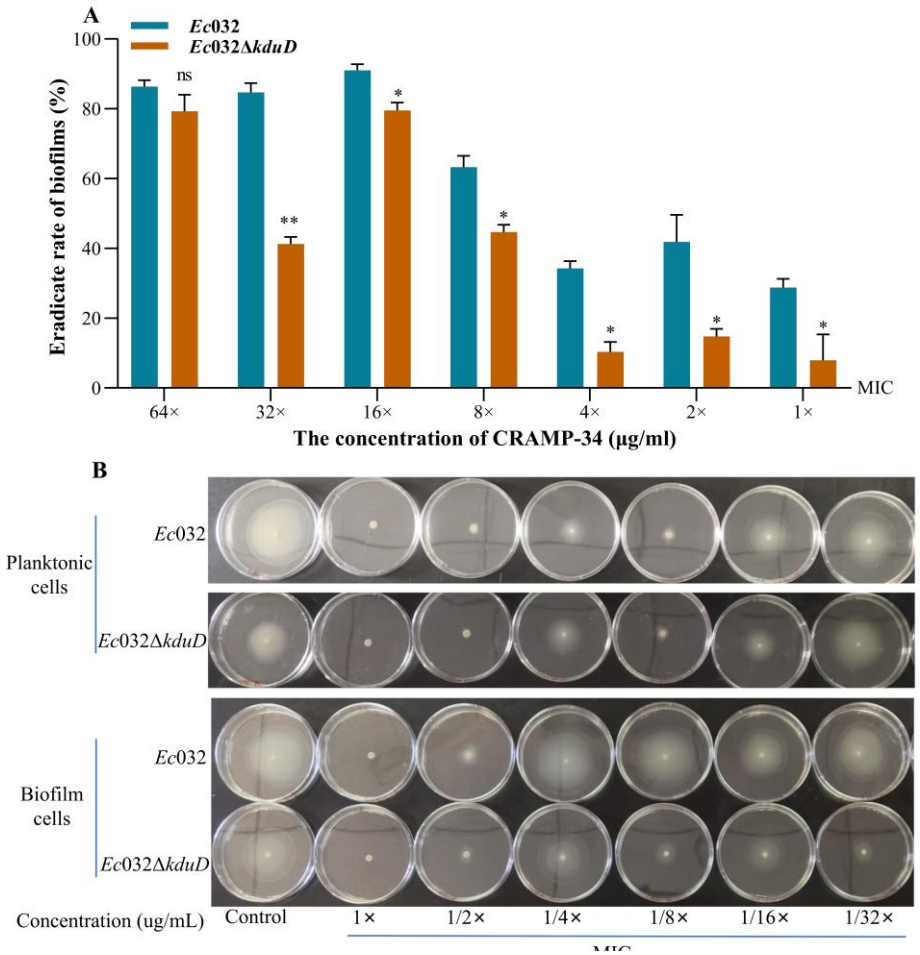

Figure 5. The inhibition rate of CRAMP-34 on 1-day-old preformed biofilms and the effect of CRAMP-34 on swimming motility. (A) The inhibition rate of CRAMP-34 on biofilms. (B) The swimming zone diameter (mm) after CRAMP-34 inhibits planktonic and biofilms bacterial swimming motility.

3. Discussion

E.coli biofilms represent a serious public and animal health concern, yet the regulatory mechanisms governing their development remain incomfully elucidated. Our previous work identified the strong biofilm-forming strain *Ec*032 from a porcine source and demonstrated that the antimicrobial peptide CRAMP-34 effectively eliminates its mature biofilms. The potent efficacy of CRAMP-34 in accelerating the healing of *E.coli*-infected full-thickness wounds underscores its therapeutic potential as a dual-function agent. The observed enhancement in wound closure and reduction in bacterial burden align with the established role of host defense peptides in modulating immune responses and directly disrupting microbial membranes. It positions CRAMP-34 not merely as a conventional AMP but as a promising anti-virulence agent that disarms a key pathogen and disrupts its community structure, thereby facilitating wound repair.

To identify key genetic determinants and assess whether CRAMP-34 targets these pathways, we performed a transposon mutagenesis screen. All 25 isolated biofilm-deficient mutants mapped to *kduD*, deletion of which severely compromised biofilms formation. As *E.coli* forms air-liquid interface biofilms—a process dependent on oxygen, flagellar motility, and cellulose, and given the established role of flagellar function in approximately half of *E.coli* biofilms mutants [13,14], we investigated motility in *Ec*032Δ*kduD*. The mutant showed markedly impaired swimming motility, despite upregulation of flagellar assembly (*fliE*, *fliA*), motor (*motA*, *motB*), and the c-di-GMP-responsive brake protein gene *ycgR*. Since *YcgR* binds c-di-GMP to mechanically inhibit flagellar rotation, its overexpression likely explains the motility defect [15]. Furthermore, upregulation of the flagellar regulatory system *qseBC* suggests that *KduD* functions within or downstream of the *QseBC* circuit,

 doi:10.20944/preprints202512.1811.v1

potentially influencing motility via c-di-GMP and *YcgR* [16]. In summary, *KduD* emerges as a novel regulator essential for biofilms formation in *Ec*032, likely through the *QseBC* system and a c-di-GMP–*YcgR*–mediated braking mechanism. Its exact molecular role and therapeutic relevance as a target of CRAMP-34 warrant further study.

Based on the established model of biofilms development—which proceeds through attachment, microcolony formation, and maturation into complex structures such as mushroom-like macrocolonies—we observed that the *Ec*032Δ*kduD* mutant retained the ability to adhere and form microcolonies, but failed to develop architecturally mature biofilms. This defect occurred despite upregulation of the key matrix genes *csgD* and *bcsA*, and a measurable increase in EPS under standardized bacterial density [17,18]. Notably, while cellulose and curli fibers—encoded by *bcsA* and *csgD*, respectively—are essential for structural integrity, particularly under nutrient limitation, their overproduction can disrupt surface adhesion and aggregation [19,20]. In *E.coli* MG1655, overexpression of *csgD* was shown to inhibit biofilms formation on hydrophobic surfaces due to excessive cellulose production [21]. Similarly, in the *Ec*032Δ*kduD* background, significant upregulation of *csgD* may drive unbalanced matrix synthesis, leading to loss of structural coordination and impaired biofilms maturation. This suggests that *KduD* contributes to biofilms integrity not by merely promoting EPS production, but by maintaining metabolic and compositional equilibrium within the matrix. In support of this, we observed concomitant upregulation of the RcsAB, a known repressor of *csgD*, likely reflecting a compensatory cellular response to restore regulatory balance [22,23]. Thus, *KduD* appears to act as a metabolic modulator whose activity fine-tunes matrix biosynthesis, ensuring the appropriate spatial and temporal deposition of polysaccharide and protein components required for stable biofilms architecture.

KduD, a 2-dehydro-3-deoxy-D-gluconate 5-dehydrogenase, participates in pentose and glucuronate metabolism [24]. Our analysis revealed that deletion of *kduD* triggered upregulation of the adjacent genes *ygeA* and *yqeF*, which are involved in glucose metabolism, indicating a compensatory metabolic adaptation. Given that *KduD* is involved in the metabolism of galacturonic and glucuronic acids [25]—key precursors for EPS biosynthesis—we hypothesize that it regulates biofilms architecture by controlling the supply of essential carbon substrates. This is supported by the observation that the *Ec*032Δ*kduD* mutant, similar to colanic acid (CA)-deficient strain, failed to form mature biofilms with the typical mushroom-like structure. CA, a branched EPS composed of glucose, galactose, and glucuronic acid, is critical for building the three-dimensional matrix of *E.coli* biofilms [26]. The inability to form structured biofilms may thus stem from a shortage of these vital EPS building blocks, impairing bacterial colonization and survival in the mammalian intestine. Furthermore, the upregulation of *ygeA*, which encodes an amino acid racemase that produces biofilm-dispersing D-amino acids, may represent a concurrent disassembly signal that further destabilizes the biofilms matrix [27,28]. In conclusion, we propose that *KduD* influences biofilms formation not through direct regulatory means but by occupying a critical metabolic node that fuels the biosynthesis of structural EPS, thereby linking central carbon metabolism to biofilms structural integrity.

Our data demonstrate that CRAMP-34 exerts potent anti-biofilm activity by inhibiting flagellar motility and eradicating mature biofilms in *Ec*032. The concomitant observation that *kduD* expression is drastically suppressed following CRAMP-34 treatment prompted us to investigate a potential functional link. The finding that CRAMP-34's biofilms clearance efficacy was significantly attenuated, though not entirely abolished, against the *Ec*032Δ*kduD* mutant provides direct genetic evidence that *KduD* is a critical target for its action. This partial persistence of activity suggests that CRAMP-34, like many effective antimicrobial peptides, employs a polypharmacological strategy, engaging multiple cellular targets to disrupt the complex biofilms network. Supporting this model, RT-qPCR analysis revealed a concerted downregulation of the *kduD*-associated metabolic operon (including *uxaA* and *uxuA*) and the glucose transporter *araE* upon CRAMP-34 treatment. This indicates a targeted disruption of a specific metabolic pathway centered on *KduD*. Furthermore, the significant suppression of the key biofilm regulators *csgD* and *bcsA* aligns with the proposed role of *KduD* in

 doi:10.20944/preprints202512.1811.v1

maintaining EPS stability and suggests a cascade of transcriptional repression. The temporal disconnect between this rapid transcriptional reprogramming and the subsequent phenotypic collapse is a hallmark of targeted anti-virulence strategies, where disabling master regulators leads to a progressive dismantling of the biofilms structure.

4. Materials and Methods

4.1. Bacterial Strains, Plasmids, Primers, and Growth Conditions

E.coli (No. *Ec*032) was isolated from porcine sources and identified as a colistin-resistant strain carrying the *mcr*-1 gene of the plasmid IncX4 with a high biofilms formation ability [1]. Bacteria were grown overnight at 37 ℃ in Brain Heart Infusion broth (BHI; Haibo Co., Ltd., Qingdao, China), harvested by centrifugation at 6 000 rpm for 10 min, and resuspended in BHI. The optical density of the bacterial suspension was measured at 600 nm (OD600 nm) and used in the subsequent experiments. The strains, plasmids, and primers are listed in Tables 1, 2 and 3, respectively.

Table 1. Bacterial strains and plasmids used in this study.

Strains/Plasmids	Description
*Ec*032	Clinical isolation of IncX4 plasmid strain carrying *mcr*-1, Colr
*Ec*032Δ	plasmid was cured
*Ec*032Δ*kduD*	*kduD* gene deletd
E. coli DH5α	cloning vectors
E. coli WM3064	a diaminopimelic acid (DAP) auxotroph strain
pCure-oriT-GFP-MCR	Aprr, oriT+, GFP+, sacB+
pCat-arr	Mariner transposon, Rifr, oriT+
pCasKp-OriT	Aprr, oriT+, bacterial expression of Cas9 nuclease and λ-Red recombination system, with temperature-sensitive replication
pSGKp-arr2	Rifr, sacB+, a sgRNA expression plasmid for targeting a specific sequence
pSGKp-*Ec*032-*kduD*	pSGKp derivative with the spacer of the *kduD* gene
pSGKp-*Ec*032-*kduD*-500	pSGKp derivative with the repair arms of the *kduD* gene

Note: Aprr, Apramycin resistant; Rifr, Rifampicin resistant; Colr, Colistin resistant; oriT+, With conjugation transfer initiation site ; sacB+, With the suicide gene sacB; GFP, With GFP fluorescent gene.

Table 2. Primer used in this study.

Primer	Sequence (5′-3′)
Eric-F	ATGTAAGCTCCTGGGGATTCAC
Eric-R	AAGTAAGTGACTGGGGTGAGCG
*Ec*032-F-XJ	GTCGAGAATTTCCGCGCTAC
*Ec*032-R-XJ	GTATTGATACCGGCACTCCG
infu-*kduD*-N20F	CACATAATCTGAAGCGCTGGGTTTTAGAGCTAGAAATAGCAAGTTAAAATAAGGC
infu-*kduD*-N20R	CCAGCGCTTCAGATTATGTGACTAGTATTATACCTAGGACTGAGCTAGC
kduD-N20-F	CACATAATCTGAAGCGCTGG
kduD-F1	TCGAATTCCTGCAGCCCGGGGGATCCTATTTACGCCCCAGGCGGAA
kduD-R1	CCGCATGGCAGGGTTTTTTA
kduD-F2	TAAAAAACCCTGCCATGCGGTATGCCCACAACTAGCGCAA
kduD-R2	TCCACCGCGGTGGCGGCCGCTCTAGATTACTGTCGATGGCCAATGC
kduD-F	TGCCGAGTGTGACCATCAAC
kduD-R	CGGAGGTTGATGTGGACGTA

 doi:10.20944/preprints202512.1811.v1

Table 3. Primers for RT-qPCR.

Gene	Forward primer sequence	Reverse primer sequence
gapA	GTTGTCGCTGAAGCAACTGG	CGATGTCCTGGCCAGCATAT
flhC	ATGCTGCCATTCTCAACCGA	GCTTGTGGGCACTGTTCAAG
fliE	GACCATTAGTTTTGCCGGGC	ACGCACCTGAATCCCCATTT
fliA	GAACGCTATGACGCCCTACA	TCCAGTTGCCCTATTGCCTG
motA	CGCCGAAACCAGCAAAATGA	TCCTCGGTTGTCGTCTGTTG
motB	TGACTGCGATGATGGCCTTT	CCCCTGGCTTTGGGTGTAAT
ycgR	GGGGCAATGGGGTGTTTTTC	CTTTGTCCGCTTTTTCCCGG
fimA	TTGTTCTGTCGGCTCTGTCC	ACTGGTTGCTCCTTCCTGTG
papG	TTCGCATCGTGAAACAGCAC	TACGTTTCGCTTCCATGGCT
csgD	GATTACCCGTACCGCGACAT	GCGTAATCAGGTAGCTGGCA
bcsA	AACGAAGGCACGCTGTTCTA	GAGGTATAGCCACGACGGTG
luxS	TTGGTACGCCAGATGAGCAG	ACGTCACGTTCCAGAATGCT
lsrK	CAGATTACTTTGGCTGGCGC	CGTAGGCCAGCCATATCCAG
qseC	CGTGACCCTGACTCGGAAAA	TTCGGTTTGCACTTTCAGCG
qseB	ATTGGCGACGGCATCAAAAC	CACGCTGACCTTTTTCTCGC
phoP	GCGCGTACTGGTTGTTGAAG	CTGGCAATCCGAGATCGACA
basS	CCTGCTGCGGATGTTATTGC	ACGCTTTACTCAACTCCCCG
basR	GTACTGATCCTCACCGCTCG	GACCCATGTTCAGCGTCAGA
rcsA	ATTGAGCCGAACCGAATCGA	GTCAGTCGGACGACATGGTA
rcsB	ATCAGTGCTGGTGGTTACGG	TCAGCAGGGCGATATCGTTC
cpxA	CGCAGGTGCCAGTTTTAACC	CAGTTCCTTGCTTTCACCGC
cpxR	TTAGTGCTGAATCCAGGCCG	CGTTTGCCCAACACTTCCTG
kduD	AACCATCGAGCAGGTCACAG	TCGCTGAACTCGAGAGCATC
uxuA	ACCAGATCGAATTCGCTGCA	CCCGGAAGACCAGCAATGAT
uxaA	GTGATTGGTCTGGGCTGTGA	CTGGCTCGCGTTTATCGTTG
araE	TTACCTGTTCGACCACCACG	GGTTTCCGGAATGAGCCAGA
ygeA	ACGATGCATAAAGTGGCGGA	AAAATTGTTCCGTCAGCCGC
yqeF	TTGCCAGCGTTGGTGTAGAT	ATTGACATTGACCCGACGCT

4.2. Determination of Minimum Inhibitory Concentration (MIC)

The MIC values of the antibiotics (Ciprofloxacin, CIP; Yuanye Co., Ltd, Shanghai, China) and Antibacterial peptides (AMPs; CRAMP-34 and LL-37; synthesized by ChinaPeptides Co., Ltd, Shanghai, China) were determined using microbroth dilution technique, as described by the Clinical and Laboratory Standards Institute (CLSI).

4.3. Biofilms Formation and Antibiofilm Assay

For the microtiter plate test (96-well plates), the mature biofilms were formed by adding 100 μL the test bacterial solution into each well of the 96-well plates and incubation at 37 ℃ for 24 h. Then, the plates were washed with phosphate-buffered saline (PBS). The two-fold dilutions of CRAMP-34, LL-37, and CIP ranging from 64 to 0.5 MICs were prepared with sterile water. Next, each antimicrobial compound was added to the corresponding plate and incubated at 37 ℃ for 3 h. The appropriate concentration of CRAMP-34 was selected and tested in a 6-well plate (Corning®3516) to confirm the results; PBS was used as a control. For selective growth of the bacteria, the following antibiotics and substances were added: 2 μg/mL colistin, 30 μg/mL apramycin, 100 μg/mL rifampin, 57 μg/mL diaminopimelic acid, 5% sucrose and 2 mg/mL L-arabinose.

4.4. Skin Wound Infection Model Was Established

The animal experiments utilized male Balb/c mice (6-8 weeks old, weighing 20-23 g, Dashuo Co., Ltd, Chengdu, China). All animal housing and handling procedures were in strict compliance with

 doi:10.20944/preprints202512.1811.v1

the Regulations for the Administration of Experimental Animals in China and were approved by the Institutional Animal Care and Use Committe of Southwest University (Permit No.: LAC2025-1-0259). Initially, the mice were subjected to general anesthesia. Subsequently, a 1-cm-diameter artificial wound was created on the dorsal surface of each mouse using surgical scissors. A volume of 200 μL of bacterial suspension (10^8 CFU/mL) was then applied to the wound site to establish a skin wound infection model. After successful establishment of the skin infection model, the mice were randomly assigned into two groups, with 10 mice per group: the PBS treatment control group infected with the *Ec*032, the CRAMP-34 treatment group infected with the *Ec*032. Throughout the treatment period, wound changes were documented daily via photography, and samples were collected for bacterial counting.

4.5. Crystal Violet Staining and Colony Count Assay

The biofilms formation assay was performed using crystal violet, and the viable bacteria were counted on trypticase soy agar plates. Briefly, the supernatant was discarded, and the cells were washed twice with sterile PBS, fixed methanol for 10 min, and stained with crystal violet for 20 min. After washing, acetic acid was used to dissolve the bound crystal violet, and the absorbance was measured at OD600 nm. To count the number of bacteria biofilms, 100 μL Triton-100X was added to disrupt the biofilms, and the bacteria were spread on TSA plates in 10-fold dilution at 37 ℃ for 12 h.

4.6. Swimming Motility Assay

LB medium plates with 0.25% (wt/vol) agar were used for the swimming motility assay. 1 μL microliter aliquots of mid-log-phase bacteria in BHI broth were spotted on a control agar plate and an agar plate containing decreasing concentrations of CRAMP. The diameters of the swimming zones were measured after incubation at 37 °C for 15 h.

4.7. Confocal Laser Scanning Microscopy (CLSM)

The morphological features of biofilms were observed by CLSM as described previously with some modifications [29]. In this experiment, 500 μL of the test bacterial solution (OD600 nm=0.1) was added to an 8-well chambered coverglass (Lab-Tek II chambered coverglass, Rochester, NY, USA), and the medium was replaced every 24 h. After incubation at 37 ℃ for 2 days, the biofilms were treated with CRAMP-34 (125 μg/mL) at 37 ℃ for 3 h, washed with 0.9% (wt/vol) NaCl, and stained at room temperature for 20 min in the dark using a Filmtracer™ LIVE/DEAD™ Biofilm Viability Kit. After rinsing with sterile water, the biofilms samples were imaged with a point-scanning confocal microscope (Eclipse Ti2; Nikon, Tokyo, Japan). The signals were recorded using the green (SYTO9, excitation of 488 nm) and red (PI, excitation of 561 nm) channels. The field of view was randomly selected under ×20 objective, and the three-dimensional image was constructed by stacking multiple images with different Z values (z-stack). The images were acquired using NIS Viewer v5.21.00 software. Four representative images were selected from each biofilms, and each experiment was repeated at least three times. The biofilm-related test parameters, such as the number, volume, base area, and fluorescence intensity, were analyzed using BiofilmQ software.

4.8. Screening of Gene Mutants with Decreased Biofilms Formation

For primary screening of the transposon library, the transconjugants were cultured to mid-log-phase, and then 5 μL was added to Corning 3595 microtiter plates containing 100 μL of BHI broth and incubated at 37 °C for 24 h. The mature biofilms were assessed by crystal violet staining. Isolates exhibiting reduced biofilms accumulation (< 75% of the wild-type level) in the primary screen were retested individually, as described previously [29]. For all reproduced mutants with a defect in biofilms accumulation, growth kinetics were evaluated based on the changes in the bacteria in BHI over a period at OD600 nm. The formation of biofilms are generally divided into four grades, the

 doi:10.20944/preprints202512.1811.v1

average OD value of negative control is defined as ODc, OD≤ODc is non-adherent, ODc<OD≤2×ODc is weakly adherent, 2×ODc <OD≤4×ODc is moderately adherent, 4×ODc <OD is strongly adherent.

4.9. Generation of a Mutagenesis Library of Ec032

E.coli WM3064 (pCure-oriT-GFP-MCR) and *Ec*032 were used as the donor (carrying Mariner transposons, with GFP fluorescent gene) and the recipient, respectively. After the donor and recipient bacteria were cultured to the logarithmic growth stage, they were conjugated at 37℃ at a ratio of 1:1 for 8-12 h. The transconjugants with GFP were selected on LB agar containing 30 μg/mL apramycin and induced in sugar-free LB broth (Yuanye Co., Ltd., Shanghai, China) with 2 mg/mL L-arabinose (Shenggong Co., Ltd., Shanghai, China) for 6 h to obtain plasmid-free *Ec*032 strain containing the pCure-oriT-GFP-MCR plasmid. These strains were cultured on LB agar plate containing 5% sucrose (Maclin Co., Ltd., Shanghai, China) at 37 ℃ for 24 h to obtain plasmid-free strain *Ec*032 (*Ec*032Δ). *E.coli* WM3064 (pCat-arr) as the donor (carrying Mariner transposons) and *Ec*032Δ as the recipient, they were conjugated at 37℃ at a ratio of 1:1 for 8-12h. We can obtain transconjugants with a total volume of 1 mL. The transconjugants were selected on LB agar containing 100 μg/mL rifampin against arr transconjugant as the positive mutant. After 100μL was diluted to a suitable gradient, the plate was coated, and the number of mutants was calculated, and the transposon mutation library was obtained.

4.10. Identification of Transposon Insertion Sites

ERIC-PCR was used to detect the contamination of the screened transposon mutants with decreased biofilms compared to *Ec*032 and *Ec*032Δ as control strains.The genomic DNA of *Ec*032 and transposon insertion mutants with reduced biofilms were extracted using the TaKaRa MiniBEST Bacteria Genomic DNA Extraction Kit Ver.3.0 (TaKaRa Co., Ltd, Beijing, China) and subjected to whole-genome sequencing at Novogene Co., Ltd. The insertion site of Mariner transposon was identified by SnapGene software and verified using primers *Ec*032-F-XJ and *Ec*032-R-XJ for PCR validation. The sequence was compared to the NCBI database to identify the gene name and base sequence for subsequent gene editing(Dou et al. 2017).

4.11. kduD Mutant Construction Using CRISPR/Cas9 System

Plasmids and genomic DNA were extracted using the TaKaRa MiniBEST Bacteria Genomic DNA Extraction Kit Ver.3.0 (Takara Biomedical Technology (Beijing) Co., Ltd., Beijing, China). In this study, we used two plasmid systems (separate expression of Cas9 and the sgRNA in pCasKp-OriT and pSGKp, respectively) for genome editing using CRISPR-Cas9 system in *E.coli* DH5α. First, the pSGKp-*Ec*032-*kduD* which encodes the sgRNA targeting the *kduD* gene (target sequence selected by SnapGene software) was constructed. Briefly, the guide RNA target sequence in pSGKp was mutagenized by PCR to target *kduD*. Primers *kduD*-F1, *kduD*-R1, *kduD*-F2 and *kduD*-R2 were used to amplify left homologous arm H1 and right homologous arm H2. pSGKp-*Ec*032-*kduD* plasmid double enzymes were cut into linea rDNA using BamHI enzyme and XbaI enzyme. The left and right homologous arms H1, H2 and linear pSGKp-*Ec*032-*kduD* plasmids were connected by NEBuilder HiFi DNA Assembly Master Mix (NEB Biological Technology (Beijing) Co., Ltd., Beijing, China) and then transformed into *E.coli* DH5α to obtain pSGKp-*Ec*032-*kduD*-500 plasmids. We performed cloning for a pSGKp-*Ec*032-*kduD*-500 plasmid harbouring a spacer (for guiding Cas9 cleavage of the wild-type *Ec*032) in *E.coli* DH5α and selected on LB plate with 100 μg/mL rifampin (Shanghai Maclin Biochemical Technology Co., Ltd., Shanghai, China). The transformants were confirmed by sequencing.

E.coli WM3064 (pCasKp-OriT) and *Ec*032 (pSGKp-*Ec*032-*kduD*-500) were used as the donor and as the recipient, respectively. After conjugation, the plasmid pCasKp-OriT from *E. coli* WM3064 was introduced into *Ec*032. The transconjugants were selected on LB agar containing 30 μg/mL apramycin (Shanghai Maclin Biochemical Technology Co., Ltd., Shanghai, China) at 30℃ for 8 h-12 h. Then the

 doi:10.20944/preprints202512.1811.v1

transconjugants were confirmed by colony PCR and DNA sequencing. The gene deletion strains were coated on 5% sucrose LB agar plate and cultured at 37 ℃ to eliminate plasmids pSGKp-*Ec*032-*kduD*-500 and pCasKp-OriT.

4.12. The Plasmid Deletion Strains Ec032ΔkduD Were Obtained

The construction of *kduD* complementation strains followed the design based on plasmid pBAD24. The *kduD* gene fragment, amplified from the genomic DNA of *Ec*032, was inserted into the multiple cloning site (MCS) of plasmid pBAD24, using ClonExpress® Ultra One Step Cloning Kit (Vazyme Biotech Co., LTD). Then, the recombinant product pBAD24-*kduD* was transformed into *E.coli* DH5α chemically competent cells and inoculated on transformed LB plates supplemented with 100 μg/mL ampicillin. Positive clones were identified through colony PCR and sequencing. Finally, the recombinant plasmid was transferred into *kduD* mutant strain via electroporation. The constructed complementation strain, named *Ec*032-Δ*kduD*/p*kduD*, induced by arabinose during culture, was used to ascertain the target of CRAMP-34 to *Ec*032.

4.13. Growth Curves

Bacteria were cultured in BHI broth to mid-log-phase and diluted to equal optical densities (OD600 nm=1). An equivalent of 200 μL of these cultures was added to 96-well microtiter plates (Corning®3599; Corning Inc., Corning, NY, USA) and incubated at 37 °C. The growth of these cultures was monitored by determining the absorbance at 600 nm every 2 h for 24 h. And OD600 nm was measured by Infinite® M Plex microplate reader (Tecan, Switzerland) after shaking. Three independent experiments were performed.

4.14. Congo Red-Binding Assay and EPS Assay

1 μL of the test bacterial suspension of *Ec*032 and *Ec*032Δ*kduD* was spotted onto 40 μg/mL Congo Red unsalt-free LB agar plate [30], which was incubated at 37 °C for 2–4 days. Subsequently, the colony morphology was compared.

EPS was determined by phenol-sulfuric acid method. The working bacterial suspension was inoculated into 6-well plate and cultivated at 37 ℃ for 24 h to form biofilms. Then, the planktonic bacteria were discarded, the well was rinsed with PBS, suspended with normal saline to scrape up the biofilms, and homogenized by repeated and even blowing. The resulting was clarified by centrifugation at 4,000 rpm, 4 ℃ for 20 min. The supernatant was filtered through a 0.22-μm filter membrane; 100 μL was added into a new centrifuge tube and mixed with 200 μL concentrated sulfuric acid and 25 μL 6% phenol solution successively for reaction in a water bath at 90 ℃ for 5 min. After cooling to room temperature, 200 μL was dispensed in a 96-well plate to measure the absorbance at the wavelength of 490 nm. Each experiment was set up in three parallel groups and repeated three times.

4.15. Real-Time Fluorescence Quantitative PCR (RT-qPCR)

The CRAMP-34 treatment of the biofilms were carried out as described above. Total RNA was extracted using Total RNA Isolation Reagent (Biosharp Co., Ltd, Beijing, China), according to manufacturer's instructions. RNA was reverse transcribed using the PrimeScript™ RT reagent Kit (TaKaRa), according to the manufacturer's instructions. Primers and probes were designed by Primer 5.0 and synthesized by Tsingke Biotechnology (Beijing, China). RT-qPCR was conducted on a CFX Connect qPCR. The reaction conditions were as follows: 95 °C for 30 s and 40 cycles of 95 °C for 5 s and 60 °C for 30 s. The relative expression levels of each target gene were computed by the 2−ΔΔCt method.

 doi:10.20944/preprints202512.1811.v1

4.16. Statistical Analysis

All experiments were conducted in triplicate, and data represented a minimum of three biological replicates. The statistical analyses were carried out using Microsoft Excel and GraphPad Prism 8.0 software. An unpaired t-test (two-tailed) was used to calculate the statistical significance. Significant differences are indicated as *($P < 0.05$), **($P < 0.01$) and ***($P < 0.001$).

5. Conclusions

This study establishes the CRAMP-34 as a potent agent capable of eradicating mature *E.coli* biofilms, its mechanism of action revealed that its efficacy is closely linked to its suppression of bacterial flagellar motility. We further identified the gene *kduD* as a novel and critical regulator governing this motility and, consequently, the entire biofilm developmental process. Therefore, our work not only highlights the therapeutic potential of CRAMP-34 but also unveils *kduD* as a central player in biofilm formation, offering a promising new target for anti-biofilm strategies.

Author Contributions: HongWei Chen, Writing-review & editing, Supervision, Project administration, Funding acquisition, Conceptualization. HongZao Yang, Writing original draft & review, Investigation, Funding acquisition, Formal analysis. Jing Xiong, Writing-original draft, Visualization, Methodology, Data curation. SiSi Su, Writing & editing, Investigation. Zhuo Yang, Visualization, Supervision, Resources. LianCi Peng, Validation, Resources. SuHui Zhang, Visualization, Software, Formal analysis. JinJie Qiu, Visualization, Software, Resources. YuZhang He, Software, Formal analysis. Wu Yang, Software, Formal analysis. All authors have read and agreed to the published version of the manuscript.

Funding: This research was funded by National Center of Technology Innovation for Pigs (NCTIP-XDB19), Yunnan Province Science and Technology Department key research development plan (202403AC100013), Chongqing Natural Science Foundation (CSTB2024NSCQ-MSX0373), Science and Technology Research Program Project of Chongqing Municipal Education Commission (KJQN20240021).

Institutional Review Board Statement: Ethical review and approval were applicable for thisstudy.

Informed Consent Statement: Not applicable.

Data Availability Statement: The original contributions presented in the study are included in the article, further inquiries can be directed to the corresponding author.

Acknowledgments: We are grateful to the National Center of Technology Innovation for Pigs for support in providing the CLSM equipment.

Conflicts of Interest: The authors declare that they have no conflicts of interest regarding the contents of this article.

Abbreviations

The following abbreviations are used in this manuscript:

E.coli	*Escherichia coli*
CRAMP-34	Cathelicidins related antimicrobial peptide
EPS	exopolysaccharides
AMP	Antibacterial peptide
PCR	Polymerase chain reaction
QS	Quorum sensing
TCS	Two omponents system
c-di-GMP	Cyclic diguanosine monophosphate
KduD	2-dehydro-3-deoxy-D-gluconate 5-dihydrogenase
CIP	Ciprofloxacin
MIC	Minimum inhibitory concentration
CLSM	Confocal Laser Scanning Microscope
RT-qPCR	Real-time fluorescent quantitative PCR

 doi:10.20944/preprints202512.1811.v1

References

1. Yang H, Liang Y, Yang Z, Liu L, Ran L, Liu J, Ma C, Wei W, Zhang S, Zhu M *et al*: Paeonol eradicates biofilm in porcine-source Escherichia coli by targeting the quorum sensing system. *BMC VET RES* 2025, 21(1):644.
2. Long J, Yang C, Liu J, Ma C, Jiao M, Hu H, Xiong J, Zhang Y, Wei W, Yang H *et al*: Tannic acid inhibits Escherichia coli biofilm formation and underlying molecular mechanisms: Biofilm regulator CsgD. *BIOMED PHARMACOTHER* 2024, 175:116716.
3. Liu L, Li H, Ma C, Liu J, Zhang Y, Xu D, Xiong J, He Y, Yang H, Chen H: Effect of anti-biofilm peptide CRAMP-34 on the biofilms of Acinetobacter lwoffii derived from dairy cows. *FRONT CELL INFECT MI* 2024, 14:1406429.
4. Ma C, Mei C, Liu J, Li H, Jiao M, Hu H, Zhang Y, Xiong J, He Y, Wei W *et al*: Effect of baicalin on eradicating biofilms of bovine milk derived Acinetobacter lwoffii. *BMC VET RES* 2024, 20(1):212.
5. Tang A, Li C, Feng D, Li A: Deciphering the code of temperature rise on aerobic granular sludge stability: A DSF-c-di-GMP mediated regulatory mechanism. *ENVIRON RES* 2025, 267:120705.
6. Perrin C, Briandet R, Jubelin G, Lejeune P, Mandrand-Berthelot M, Rodrigue A, Dorel C: Nickel promotes biofilm formation by Escherichia coli K-12 strains that produce curli. *APPL ENVIRON MICROB* 2009, 75(6):1723-1733.
7. Manobala T: Peptide-based strategies for overcoming biofilm-associated infections: a comprehensive review. *CRIT REV MICROBIOL* 2025, 51(4):563-580.
8. Gong H, He L, Zhao Z, Mao X, Zhang C: The specific effect of (R)-(+)-pulegone on growth and biofilm formation in multi-drug resistant Escherichia coli and molecular mechanisms underlying the expression of pgaABCD genes. *BIOMED PHARMACOTHER* 2021, 134:111149.
9. Shi Z, Zhai J, Yu J, Wang Z, Liu H, Yang X, Wang X: Biofilm formation by Gallibacterium anatis depends on TolC-mediated initial attachment of cells. *Veterinary journal (London, England : 1997)* 2025, 314:106488.
10. Dweba Y, Eleojo Aruwa C, Sabiu S: In Silico Bioprospection of Daniellia oliveri-Based Products as Quorum Sensing Modulators of Escherichia coli SdiA. *BIOCHEM RES INT* 2025, 2025:7191508.
11. Niu N, Dou L, Yang S, Wang H, Zhuang S, Fan Y, Liu Y, Zhang W, Ma W: Drug resistance detection of canine origin Escherichia coli in China and inhibition by genipin. *Veterinary journal (London, England : 1997)* 2025, 310:106307.
12. Wang S, Ma C, Long J, Cheng P, Zhang Y, Peng L, Fu L, Yu Y, Xu D, Zhang S *et al*: Impact of CRAMP-34 on Pseudomonas aeruginosa biofilms and extracellular metabolites. *FRONT CELL INFECT MI* 2023, 13:1295311.
13. Wang Z, Tang Y, Li H, Li J, Chi X, Ma X, Liu Z: ArgR regulates motility and virulence through positive control of flagellar genes and inhibition of diguanylate cyclase expression in Aeromonas veronii. *COMMUN BIOL* 2024, 7(1):1720.
14. Sun G, Yu Z, Li Q, Zhang Y, Wang M, Liu Y, Liu J, Liu L, Yu X: Mechanism of Escherichia coli Lethality Caused by Overexpression of flhDC, the Flagellar Master Regulator Genes, as Revealed by Transcriptome Analysis. *International journal of molecular sciences* 2023, 24(18):14058.
15. Visnardi AB, Ribeiro RA, de Souza AS, Churasacari Vinces TG, Llontop EE, de Almeida Ferrari AS, França Henrique PA, Valdivieso D, Sánchez-Limache DE, Silva GR *et al*: Insertion of a Divergent GAF-like Domain Defines a Novel Family of YcgR Homologues That Bind c-di-GMP in Leptospirales. *ACS OMEGA* 2025, 10(4):3988-4006.
16. Chen Y, Liu Z, Chen B, Tam H, Shia W, Yu H, Chen P: Effects of Heat-Killed Probiotic Strains on Biofilm Formation, Transcription of Virulence-Associated Genes, and Prevention of UTIs in Mice. *PROBIOTICS ANTIMICRO* 2025, 17(6):4619-4634.
17. Wang Y, Zhang R, Wang P, Zhang W, Li Z, Pang X, Huang F, Wang S, Liu X, Zhang H: Biofilm-mediated resistance to berberine in Escherichia coli. *FRONT CELL INFECT MI* 2025, 15:1565714.
18. Chen S, Feng Z, Sun H, Zhang R, Qin T, Peng D: Biofilm-Formation-Related Genes csgD and bcsA Promote the Vertical Transmission of Salmonella Enteritidis in Chicken. *FRONT VET SCI* 2021, 7:625049.
19. Li S, Bi C, Xiang B, Wang Z, Yang H, Fu C, Chen L, Chen Y: The role of cyclic di-GMP in biomaterial-associated infections caused by commensal Escherichia coli. *PLOS ONE* 2025, 20(8):e330229.

 doi:10.20944/preprints202512.1811.v1

20. Shrestha S, Bista S, Byanjankar N, Prasai Joshi T: Evaluation of bottled drinking water and occurrence of multidrug-resistance and biofilm producing bacteria in Nepal. *Environmental pollution (Barking, Essex : 1987)* 2024, 341:122896.
21. Li F, Cao L, Bähre H, Kim S, Schroeder K, Jonas K, Koonce K, Mekonnen SA, Mohanty S, Bai F *et al*: Patatin-like phospholipase CapV in Escherichia coli - morphological and physiological effects of one amino acid substitution. *NPJ BIOFILMS MICROBI* 2022, 8(1):39.
22. Vianney A, Jubelin G, Renault S, Dorel C, Lejeune P, Lazzaroni JC: Escherichia coli tol and rcs genes participate in the complex network affecting curli synthesis. *Microbiology (Reading, England)* 2005, 151(Pt 7):2487-2497.
23. Chen C, Nguyen LT, Cottrell BJ, Irwin PL, Uhlich GA: Multiple mechanisms responsible for strong Congo-red-binding variants of Escherichia coli O157:H7 strains. *PATHOG DIS* 2016, 74(2):ftv123.
24. Tubeleviciute A, Teese MG, Jose J: Escherichia coli kduD encodes an oxidoreductase that converts both sugar and steroid substrates. *APPL MICROBIOL BIOT* 2014, 98(12):5471-5485.
25. Maruyama Y, Oiki S, Takase R, Mikami B, Murata K, Hashimoto W: Metabolic fate of unsaturated glucuronic/iduronic acids from glycosaminoglycans: molecular identification and structure determination of streptococcal isomerase and dehydrogenase. *The Journal of biological chemistry* 2015, 290(10):6281-6292.
26. Hwang Y, Perez M, Holzel R, Harshey RM: c-di-GMP is required for swarming in E. coli, producing colanic acid that acts as surfactant. *MBIO* 2025, 16(6):e91625.
27. Hodge-Hanson KM, Zoino A, Downs DM: Expression of Pyridoxal 5'-Phosphate-Independent Racemases Can Reduce 2-Aminoacrylate Stress in Salmonella enterica. *J BACTERIOL* 2018, 200(9):e717-e751.
28. Miyamoto T, Saitoh Y, Katane M, Sekine M, Homma H: YgeA is involved in L- and D-homoserine metabolism in Escherichia coli. *FEMS MICROBIOL LETT* 2022, 369(1):fnac96.
29. Zhang Y, Cheng P, Wang S, Li X, Peng L, Fang R, Xiong J, Li H, Mei C, Gao J *et al*: Pseudomonas aeruginosa biofilm dispersion by the mouse antimicrobial peptide CRAMP. *VET RES* 2022, 53(1):80.
30. Monikadevi G, Vijayakumar S, Vanathi P, Prathipkumar S, Al-Sadoon MK, Srinivasan P, Vidhya E: Fruit Extract Mediated Formation of Luminescent Titanium Dioxide Nanometer-Sized Particles: An Innovative Strategy in Domain of Photodecomposition and Germicidal Properties. *LUMINESCENCE* 2024, 39(11):e70025.